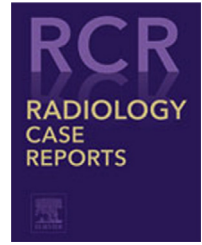


Available online at [www.sciencedirect.com](http://www.sciencedirect.com)

ScienceDirect

journal homepage: [www.elsevier.com/locate/radcr](http://www.elsevier.com/locate/radcr)

## Case report

## Pulmonary hamartoma: Feasibility of dual-energy CT detection of intranodular fat

Koji Takumi, MD, PhD<sup>a,\*</sup>, Hiroaki Nagano, MD<sup>a</sup>, Tomohiro Harasawa, MD<sup>a</sup>, Kazuhiro Tabata, MD, PhD<sup>b</sup>, Takuya Tokunaga, MD<sup>c</sup>, Takashi Yoshiura, MD, PhD<sup>a</sup>

<sup>a</sup> Departments of Radiology, Kagoshima University Graduate School of Medical and Dental Sciences, 8-35-1 Sakuragaoka, Kagoshima City, 890-8544, Japan

<sup>b</sup> Human Pathology, Kagoshima University Graduate School of Medical and Dental Sciences, 8-35-1 Sakuragaoka, Kagoshima City, 890-8544, Japan

<sup>c</sup> General Thoracic Surgery, Kagoshima University Graduate School of Medical and Dental Sciences, 8-35-1 Sakuragaoka, Kagoshima City, 890-8544, Japan

## ARTICLE INFO

## Article history:

Received 7 January 2021

Revised 29 January 2021

Accepted 31 January 2021

## Keywords:

Pulmonary hamartoma

Dual-energy computed tomography (CT)

Fat

## ABSTRACT

We have reported 2 cases of pulmonary hamartoma focusing on detecting intranodular fat, which is one of CT features suggestive of pulmonary hamartoma, using dual-energy CT analyses. For patient 1, a 73-year-old man was pointed out to have a nodular opacity on chest radiograph of pretreatment workup for retinal detachment. In patient 2, a 66-year-old woman with uterine carcinoma admitted for preoperative assessment. Both patients underwent dual-energy CT examination and the pulmonary lesions exhibited a downward-sloping curve at lower X-ray energies on attenuation curve of virtual monochromatic images, which suggested fatty tissue. Dual-energy CT analysis can help diagnose pulmonary hamartoma with detection of intralesional fatty tissue.

© 2021 The Authors. Published by Elsevier Inc. on behalf of University of Washington.

This is an open access article under the CC BY-NC-ND license (<http://creativecommons.org/licenses/by-nc-nd/4.0/>)

### Introduction

Pulmonary hamartoma is the most common benign tumor of the lung accounting for approximately 6%–8% of primary lung tumors and 75% of all benign lesions [1–3]. Accurate diagnosis of pulmonary hamartoma facilitates less invasive lung resection such as tumor enucleation. Diagnosis of pulmonary hamartoma by fine needle aspiration cytology has been reported to show 78% specificity and 22% false-positive rate [4] and be more difficult to diagnose compared to malignant

tumors. Therefore, there is a compelling need for radiological imaging approach to improve diagnostic accuracy. CT features suggestive of pulmonary hamartoma include intranodular fat and popcorn-like calcifications [5]. Dual-energy CT has been introduced in clinical practice, and can obtain information about tissue composition by evaluating material-specific attenuation behavior at different X-ray energy levels [6,7]. CT attenuation changes on dual-energy CT analysis have been reported to be useful for diagnosing adrenal adenomas and cholesterol gallstones by detecting intralesional fat or cholesterol [8,9]. However, to our knowledge, dual-energy CT analysis

\* Corresponding author.

E-mail address: [takumi@m2.kufm.kagoshima-u.ac.jp](mailto:takumi@m2.kufm.kagoshima-u.ac.jp) (K. Takumi).

<https://doi.org/10.1016/j.radcr.2021.01.062>

1930-0433/© 2021 The Authors. Published by Elsevier Inc. on behalf of University of Washington. This is an open access article under the CC BY-NC-ND license (<http://creativecommons.org/licenses/by-nc-nd/4.0/>)

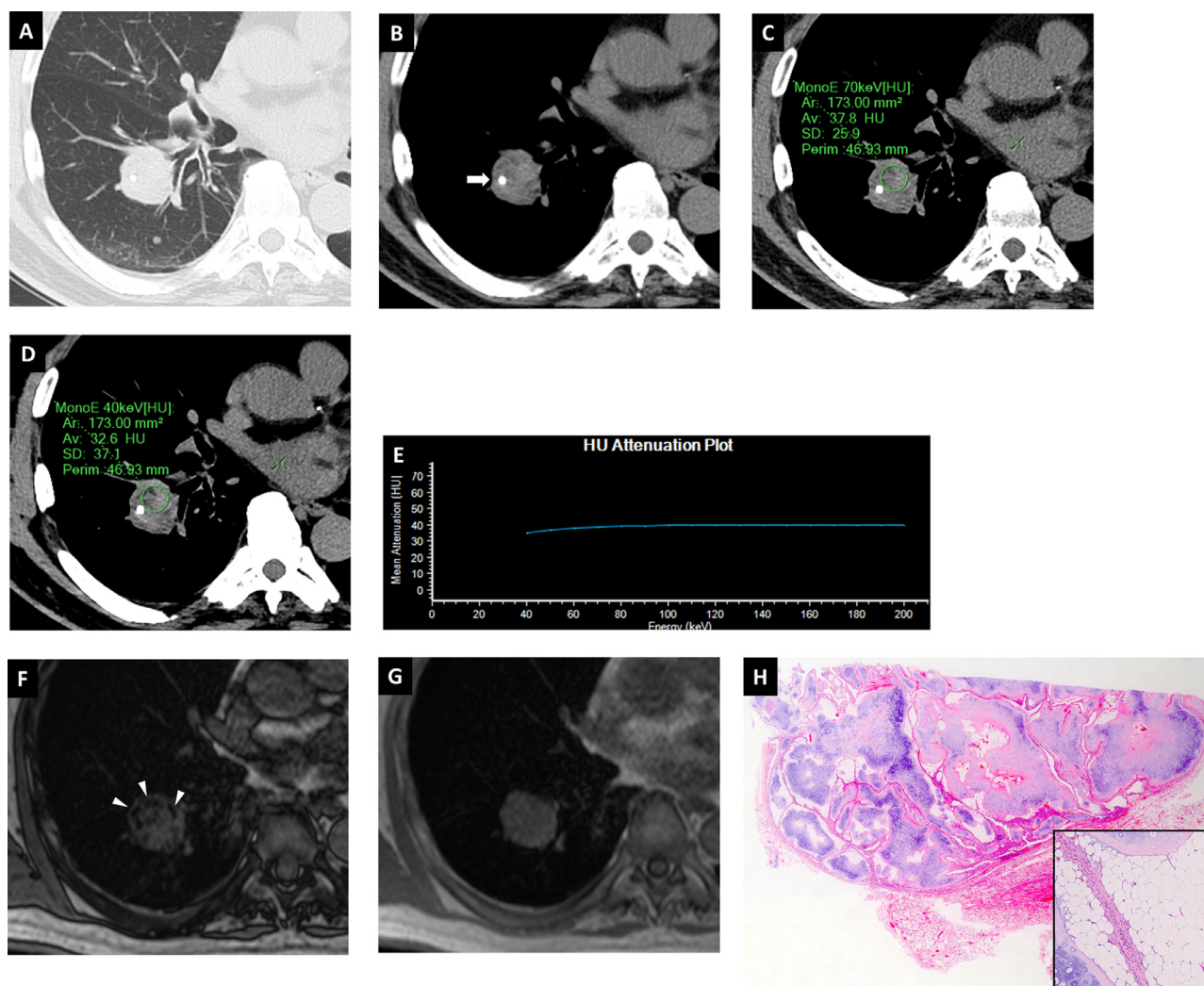


**Fig. 1** – Case 1 - Axial lung window (A) and soft tissue window (B) CT images demonstrate a well-defined and heterogeneous solitary pulmonary lesion with calcification measuring 35 mm in diameter in the right lower lobe (arrow). The mean Hounsfield unit on 40 keV virtual monochromatic image (D) is lower than that on 70 keV virtual monochromatic image (C) (32.6 vs. 37.8 HU). Attenuation curve of virtual monochromatic images (E) exhibited a downward-sloping curve at lower X-ray energies. In-phase MR image (G) shows low signal intensity of nodule and out-of-phase image (F) shows loss of signal (arrowheads) in the nodule. Microscopically, it shows that the tumor consists of mature cartilage with adipose tissue (right lower corner) and fibrovascular without bronchial glands (H).

for detection of intranodular fat in pulmonary hamartoma has never been reported.

## Case report

### Case 1

A 73-year-old man visited our hospital for pretreatment workup for retinal detachment. Chest radiograph demonstrated a nodular opacity within the right middle lung zone. The patient underwent chest CT for further evaluation, which was performed using a dual-layer spectral CT (IQon spectral CT; Philips Healthcare, Best, the Netherlands). Imaging

parameters were as follows: tube voltage, 120 kVp; gantry rotation time, 0.4 s; effective tube current-time product, 160 mAs with auto-modulation; pitch, 0.703; and detector row configuration, 64 × 0.625 mm. Dual-energy analyses were performed with a thinclient workstation (Spectral Diagnostic Suite; Philips Healthcare). Unenhanced conventional CT demonstrated a well-defined and round-shape mass measuring 35 mm located the right lower lobe (Fig. 1A and B). The mean attenuation of the lesion was 35.9 HU with some low attenuation pixels less than 0 HU. Virtual monochromatic images (VMIs) using dual-energy analysis revealed decrease in attenuation as the tube voltage decreased (Fig. 1C-E). On chemical-shift MR imaging, lower signal intensity in the lesion was shown on an out-of-phase image (TR/TE/FA/ETL, 200/1.38/65°/2) (Fig. 1F) compared with an in-phase image

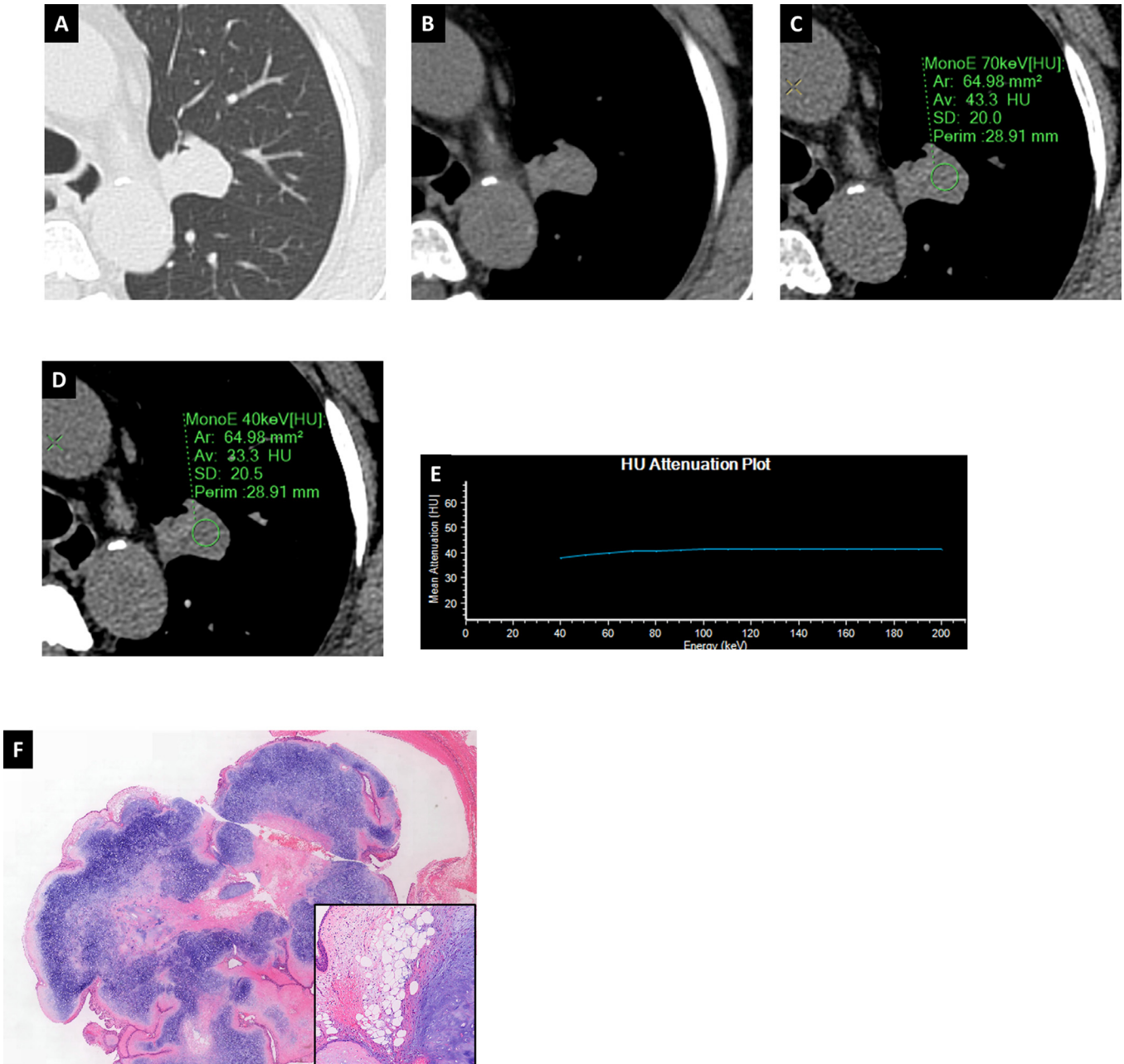


**Fig. 2 – Case 2 - Axial lung window (A) and soft tissue window (B) CT images demonstrate a well-defined and homogeneous solitary pulmonary nodule without calcification measuring 23 mm in diameter in the left upper lobe. The mean Hounsfield unit on 40 keV VMI (D) is lower than that on 70 keV VMI (C) (33.3 vs. 43.3 HU). Attenuation curve of virtual monochromatic images (E) exhibited a downward-sloping curve at lower X-ray energies. Microscopically, it shows that a variety of mesenchymal elements, including hyaline cartilage, fibrovascular stroma, bronchial glands (F), small amount of adipose tissue is also seen (right lower corner).**

(TR/TE/FA/ETL, 200/2.46/65°/2) (Fig. 1G), which suggested presence of intranodular fat component. With those radiological findings, the lesion was diagnosed as a pulmonary hamartoma. The patient opted to have a surgery, and the lesion was completely resected. The tumor was histopathologically diagnosed as a pulmonary hamartoma with the presence of fatty tissue (Fig. 1H).

#### Case 2

A 66-year-old woman with uterine carcinoma was admitted to our hospital for preoperative assessment. Unenhanced conventional chest CT demonstrated a round and regular-margined iso-attenuation nodule measuring 23 mm located left upper lobe (Fig. 2A and B). The mean attenuation of the

nodule was 43.6 HU without low attenuation pixels less than 0 HU. VMIs revealed decrease in attenuation as tube voltage decreased (Fig. 2C-E). These CT findings along with the clinical history suggested a differential diagnosis of benign hamartoma versus metastatic uterine carcinoma. A decision to obtain histopathological confirmation was made as metastatic tumor could not be completely excluded. Histological examination revealed a pulmonary hamartoma with fatty component (Fig. 2E).

## Discussion

Our two cases showed rounded small masses (<4cm) with smooth margin and the case 1 had intralesional calcification. Those findings were suggestive of a pulmonary hamartoma, but other benign lesions or malignancies including metastatic lung tumors stayed in the differential diagnosis list as they could show similar imaging appearances.

Evaluation of fat content based on conventional CT Hounsfield unit has been widely used to diagnose variety of lesions such as hepatic steatosis [10] and adrenal adenomas [11]. Likewise, presence of detectable intralesional fatty tissue on conventional CT is helpful for diagnosis of pulmonary hamartoma [2]. However, it has been reported that only 50% of pulmonary hamartomas have fat deposits that is detectable on conventional CT images [2]. Case 1 had measurable low attenuation pixels within the lesion which suggested fatty tissue. On the other hand, the low attenuation area was not detected in case 2. Chemical shift MR imaging is a well-established and sensitive method to detect a small amount of fat [12-15]. In case 1, signal intensity drop on out-of-phase images compared to in-phase images correctly predicted the presence of a fat component.

Dual-energy CT analysis for evaluation of tissue characteristics relies on the unique CT attenuation properties of different materials at different tube voltage settings. Fat tissue has been reported to exhibit unique CT attenuation changes with decrease in attenuation at lower kV images than higher ones [16]. For diagnosing adrenal lesions, Gupta et al. [8] reported that identifying a decrease in the density of the adrenal lesion from higher to lower kV images can be an indicator of intralesional fat component. The presented 2 cases demonstrated highest HU values at high keV, with monotonic decreases at lower keV, matching the expected behavior of fatty tissue. Nonetheless, it should be noted that these CT attenuation changes depend on the amount of fat within the lesion [8]. Pulmonary hamartomas with low fat content could be difficult to diagnose with radiological approach including dual-energy CT analyses. Further research is desirable to evaluate the diagnostic accuracy for pulmonary hamartoma using dual-energy CT analysis.

This report highlights a novel approach to diagnosing pulmonary hamartomas by using dual-energy CT analysis. The intranodular fat detected by dual-energy CT may help diagnose pulmonary hamartoma.

## Patient consent statement

Informed consent was waived off, as ours is a retrospective study and patient identifying details are not revealed in entire manuscript.

## REFERENCES

- [1] Wiatrowska BA, Yazdi HM, Matzinger FR, MacDonald LL. Fine needle aspiration biopsy of pulmonary hamartomas. Radiologic, cytologic and immunocytochemical study of 15 cases. *Acta Cytol* 1995;39:1167–74.
- [2] Siegelman SS, Khouri NF, Scott WW Jr, Leo FP, Hamper UM, Fishman EK, et al. Pulmonary hamartoma: CT findings. *Radiology* 1986;160:313–17. doi:10.1148/radiology.160.2.3726106.
- [3] De Cicco C, Bellomi M, Bartolomei M, Carbone G, Pelosi G, Veronesi G, et al. Imaging of lung hamartomas by multidetector computed tomography and positron emission tomography. *Ann Thoracic Surg* 2008;86:1769–72. doi:10.1016/j.athoracsur.2008.08.033.
- [4] Hughes JH, Young NA, Wilbur DC, Renshaw AA, Mody DR. Fine-needle aspiration of pulmonary hamartoma: a common source of false-positive diagnoses in the College of American Pathologists Interlaboratory Comparison Program in Nongynecologic Cytology. *Arch Pathol & Laboratory Med* 2005;129:19–22.
- [5] Hochhegger B, Nin CS, Alves GRT, Hochhegger DR, de Souza VVS, Watte G, et al. Multidetector computed tomography findings in pulmonary hamartomas: a new fat detection threshold. *J Thoracic Imaging* 2016;31:11–14. doi:10.1097/RTI.0000000000000180.
- [6] Kalender WA, Perman WH, Vetter JR, Klotz E. Evaluation of a prototype dual-energy computed tomographic apparatus. I. Phantom studies. *Medical physics* 1986;13:334–9. doi:10.1118/1.595958.
- [7] Alvarez RE, Macovski A. Energy-selective reconstructions in X-ray computerized tomography. *Physics in Med Biol* 1976;21:733–44. doi:10.1088/0031-9155/21/5/002.
- [8] Gupta RT, Ho LM, Marin D, Boll DT, Barnhart HX, Nelson RC. Dual-energy CT for characterization of adrenal nodules: initial experience. *AJR. Am J Roentgenol* 2010;194:1479–83. doi:10.2214/ajr.09.3476.
- [9] Yang CB, Zhang S, Jia YJ, Duan HF, Ma GM, Zhang XR, et al. Clinical application of dual-energy spectral computed tomography in detecting cholesterol gallstones from surrounding bile. *Acad Radiol* 2017;24:478–82. doi:10.1016/j.acra.2016.10.006.
- [10] Kodama Y, Ng CS, Wu TT, Ayers GD, Curley SA, Abdalla EK, et al. Comparison of CT methods for determining the fat content of the liver. *AJR. Am J Roentgenol* 2007;188:1307–12. doi:10.2214/AJR.06.0992.
- [11] Catalano OA, Samir AE, Sahani DV, Hahn PF. Pixel distribution analysis: can it be used to distinguish clear cell carcinomas from angiomyolipomas with minimal fat? *Radiology* 2008;247:738–46. doi:10.1148/radiol.2473070785.
- [12] Ozturk K, Soylu E, Yazici Z, Ozkaya G, Savci G. Differentiation of hepatocellular carcinoma from non-hepatocellular malignant tumours of liver by chemical-shift MRI at 3 T. *Clin Radiol* 2019;74:797–804. doi:10.1016/j.crad.2019.06.006.

- [13] Outwater EK, Bhatia M, Siegelman ES, Burke MA, Mitchell DG. Lipid in renal clear cell carcinoma: detection on opposed-phase gradient-echo MR images. *Radiology* 1997;205:103–7. doi:[10.1148/radiology.205.1.9314970](https://doi.org/10.1148/radiology.205.1.9314970).
- [14] Fujiyoshi F, Nakajo M, Fukukura Y, Tsuchimochi S. Characterization of adrenal tumors by chemical shift fast low-angle shot MR imaging: comparison of four methods of quantitative evaluation. *AJR. Am J Roentgenol* 2003;180:1649–57. doi:[10.2214/ajr.180.6.1801649](https://doi.org/10.2214/ajr.180.6.1801649).
- [15] Hochegger B, Marchiori E, dos Reis DQ, Souza AS Jr, Souza LS, Brum T, et al. Chemical-shift MRI of pulmonary hamartomas: initial experience using a modified technique to assess nodule fat. *AJR. Am J Roentgenol* 2012;199:W331–4. doi:[10.2214/ajr.11.8056](https://doi.org/10.2214/ajr.11.8056).
- [16] Zheng X, Ren Y, Phillips WT, Li M, Song M, Hua Y, Zhang G. Assessment of hepatic fatty infiltration using spectral computed tomography imaging: a pilot study. *J Computer Assisted Tomography* 2013;37:134–41. doi:[10.1097/RCT.0b013e31827ddad3](https://doi.org/10.1097/RCT.0b013e31827ddad3).